Volume 147 Number 13 7 July 2022 Pages 2873-3120

Analyst

rsc.li/analyst



ISSN 0003-2654



PAPER

Abhishek Jain *et al.*Intracellular calcium dynamics of lymphatic endothelial and muscle cells co-cultured in a Lymphangion-Chip under pulsatile flow

Analyst



PAPER



Cite this: Analyst, 2022, 147, 2953

Intracellular calcium dynamics of lymphatic endothelial and muscle cells co-cultured in a Lymphangion-Chip under pulsatile flow†

The lymphatic vascular function is regulated by pulsatile shear stresses through signaling mediated by intracellular calcium [Ca²⁺]_i. Further, the intracellular calcium dynamics mediates signaling between lymphatic endothelial cells (LECs) and muscle cells (LMCs), including the lymphatic tone and contractility. Although calcium signaling has been characterized on LEC monolayers under uniform or step changes in shear stress, these dynamics have not been revealed in LMCs under physiologically-relevant co-culture conditions with LECs or under pulsatile flow. In this study, a cylindrical organ-on-chip platform of the lymphatic vessel (Lymphangion-Chip) consisting of a lumen formed with axially-aligned LECs co-cultured with transversally wrapped layers of LMCs was exposed to step changes or pulsatile shear stress, as often experienced in vivo physiologically or pathologically. Through real-time analysis of intracellular calcium [Ca²⁺]_i release, the device reveals the pulsatile shear-dependent biological coupling between LECs and LMCs. Upon step shear, both cell types undergo a relatively rapid rise in [Ca²⁺]_i followed by a gradual decay. Importantly, under pulsatile flow, analysis of the calcium signal also reveals a secondary sinusoid within the LECs and LMCs that is very close to the flow frequency. Finally, LMCs directly influence the LEC calcium dynamics both under step changes in shear and under pulsatile flow, demonstrating a coupling of LEC-LMC signaling. In conclusion, the Lymphangion-Chip is able to illustrate that intracellular calcium [Ca²⁺]_i in lymphatic vascular cells is dependent on pulsatile shear rate and therefore, serves as an analytical biomarker of mechanotransduction within LECs and LMCs, and functional consequences.

Received 7th March 2022, Accepted 25th May 2022 DOI: 10.1039/d2an00396a

rsc.li/analyst

Introduction

The lymphatic vascular system within circulation has a crucial role in maintaining body fluid, lipid absorption, protein balance, and immune cell transport.^{1–3} Using intrinsic and extrinsic contractility, the lymphatic vessel's functional unit (lymphangion) collects and returns the interstitial fluid to the circulatory system while its dysfunction leads to interstitial fluid accumulation (*i.e.* lymphedema), fibrosis, and inflammation.^{4–7} The mechanical forces such as shear stress due to lymph flow are known to be uniquely complex and pul-

satile and have a profound effect on lymphangion's activity including permeability, contraction, tone, and frequency.8-11 Further, the lymphatic endothelial cells (LECs) and muscle cells (LMCs) operate as a unit and the cellular crosstalk between these cell types regulates the mechanical and biological functions of the lymphatic vessels in both health and disease. Notably, the shear-induced activation of a variety of cell-surface receptors by vasoactive agents - such as, nitric oxide (NO)12,13 or endothelin-114,15 - is tightly coupled with the elevation of intracellular calcium, 16,17 which serves as one of the major players and secondary messengers in shear-activated vascular signaling. 18 Within blood vessels, it is well known that endothelial-derived hyperpolarization caused by an elevation in the intracellular Ca²⁺ concentration functions as a signaling pathway between endothelial cells (EC) as well as between ECs and smooth muscle cells (SMCs). 19,20 This signaling passes through the endothelial gap junction and spreads a wave through the vessel leading to vasodilation and contractile modulation.²¹ Although there is extensive available literature on mechanical shear stress effect in blood vessels and the interconnected intracellular calcium signaling, there

^aDepartment of Biomedical Engineering, College of Engineering, Texas A&M University, College Station, TX, USA. E-mail: a.jain@tamu.edu;

Fax: +1 979 845 5532; Tel: +1 979 458 8494

^bDepartment of Medical Physiology, College of Medicine, Texas A&M Health Science Center, Bryan, TX, USA

^cDepartment of Cardiovascular Sciences, Houston Methodist Academic Institute, Houston TX USA

[†] Electronic supplementary information (ESI) available. See DOI: https://doi.org/ 10.1039/d2an00396a

is little known regarding such dynamics within lymphatics. Importantly, the prior work that characterized shear-dependent calcium and electrical dynamics in LECs showed a unique mechanosensitivity in these cells compared to the blood vascular ECs. 22-26 In LECs, shear-mediated calcium signal has been shown to be dependent on the magnitude of the shear and is dependent on calcium release as well as entry of extracellular calcium (22). Further, analysis of cytosolic Ca²⁺ using cannulated rat/mouse lymphatic vessel has shown the influence of calcium flash within the living vessel, but these data cannot specifically show the independent or coupled role of LECs and LMCs individually, ^{27,28} due to the complex nature of the in vivo models, small size and the technical difficulty to separate the two cell types in a functional lymphatic vessel.²⁹ There have been no studies that measured the possibly unique intracellular calcium dynamics of the LECs and LMCs co-cultured in a physiologically-relevant architecture or under the

influence of pulsatile lymph flow. 10,30,31 Consequently, there is little knowledge on the extent of functional coupling between the LECs and the LMCs relative to the blood vessel. We recently introduced and characterized Lymphangion-Chip as a microphysiological system which supports co-culture and bidirectional signaling of lymphatic endothelial and muscle cells³² (Fig. 1A). In this device, a monolayer of axially-aligned endothelial lumen surrounded by multiple and uniformly thick layers of circumferentially-oriented muscle cells can be co-cultured for several days under flow, as only observed in vivo in the past. In this work, we integrated this device to a step change and pulsatile flow control system, and measured the independent and coupled intracellular calcium dynamics within LECs and LMCs that is physiologically-relevant (Fig. 1B, C and ESI Video 1†). Our findings reveal the differential regulation of flow profile and LMC-LEC coupling in shearmediated lymphatic functions. We propose that intracellular

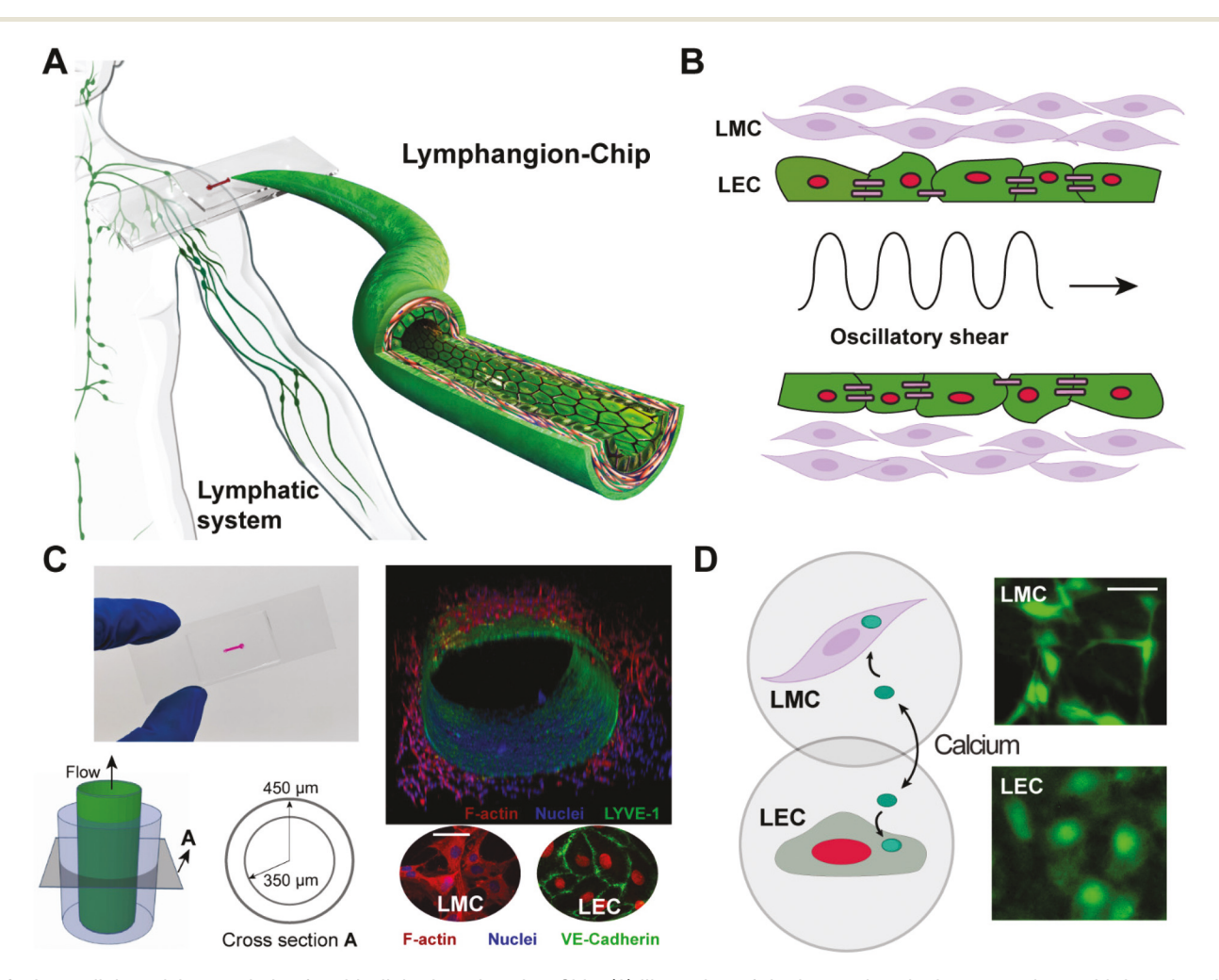


Fig. 1 Intracellular calcium analysis of multicellular Lymphangion-Chip. (A) Illustration of the human lymphatic system along with Lymphangion-Chip as a microfluidic device to include living co-culture lymphatic endothelial cells (LECs) and lymphatic muscle cells (LMCs). (B) Infographic describing on-chip co-culture of LECs surrounded by LMCs to study intracellular calcium content within lymphatic cells under oscillatory shear profile. (C) A picture of the fabricated devices along with 3D illustration and confocal micrograph of Lymphangion-Chip consisting of co-culture of LECs and LMCs (top image, green: LYVE-1, red: F-actin, blue: nuclei; bottom image, green: VE-Cadherin, red: F-actin, blue: nuclei) (D) illustration of calcium signaling in LECs and LMCs along with the representative fluorescent images to show the real-time measurement of intracellular calcium within lymphatic cells (green: cytosolic calcium). Scale bars: 20 μm.

Ca²⁺calcium may serve as a specific biomarker of mechanotransduction within LECs and LMCs, and functional consequences (Fig. 1D).

Methods

Lymphangion-Chip design

The microfluidic devices were fabricated using soft lithography of polydimethylsiloxane (PDMS, Dow Corning) as previously described.32,33 In summary, the mold with a 5 mm long channel and 900 μ m \times 900 μ m cross-section was designed using SolidWorks and 3D printed with Eden350 setup. PDMS mixture (1:10 base to cross-linker ratio) was poured and cured in the mold and after removing the slab, inlet and outlets were punched with a 1 mm biopsy punch (Ted Pella). Then, the microfluidic devices were fabricated by binding slabs to PDMS-coated glass slides. We treated the devices with oxygenplasma (120 Watts, Thierry Zepto, Diener Electronics) followed by silanizing (10% v/v of (3-aminopropyl) trimethoxysilane in ethanol, Sigma-Aldrich) for 15 minutes. Then, the devices were washed extensively with 100% ethanol followed by 70% ethanol and kept in an 80° oven for 2 hours. Later, the devices were filled with 2.5% v/v glutaraldehyde (Sigma-Aldrich) for 15 minutes and washed with 70% ethanol followed by a final 2 hours drying step in an 80 °C oven.

Lymphatic cell culture using gravitational lumen patterning

We isolated LECs and LMCs from rat mesenteric lymphatic vessel using a previously published technique.34,35 In brief, two rat mesenteric lymphatic vessels were dissected and incubated on two gelatin-coated plastic culture dishes. To isolate LECs, one of the vessels was inverted before placing on the culture dish. Meanwhile, for LMCs isolation, the dissected vessel was attached to the plastic tissue culture by gently pressing it onto the surface with forceps. Both dishes were filled with high-glucose Dulbecco's modified Eagle's medium (DMEM) supplemented with 20% FBS, 2 mM sodium pyruvate, 2 mM L-glutamine, and antibiotics and were placed in 5% and 10% CO₂ for LECs and LMCs isolation, respectively. After 3-4 days, the cells were proliferated and migrated out of the vessel. At this stage, the vessels were removed, and LECs and LMCs were first recognized based on morphology and then with the uptake of fluorescent acetylated-LDL which is taken up specifically by endothelial cells via the "scavenger cell pathway" of LDL metabolism (identification and isolation of endothelial cells based on their increased uptake). The LMC phenotype was also confirmed on the criteria of 95% expression of specific markers of α -SMA and SM-22a. When the phenotype of the cells was confirmed, the undesired cells were destroyed physically and the target cells (either LMCs or LECs) were kept to grow and fill the plate's surface. The rat cell isolation protocols were all approved by the Texas A&M University Laboratory Animal Care Committee (IACUC 2019-0284). LECs were kept in 99% v/v Endothelial Cell Growth Medium MV2 (full supplemental kit, PromoCell) and 1% v/v antibiotic cocktail

(Gibco) in a humidified 37° and 5% $\rm CO_2$ incubator while LMCs were cultured in 89% v/v DMEM/F-12 (Gibco), 10% v/v FBS (Gibco) and 1% v/v antibiotic cocktail in a 10% $\rm CO_2$ incubator.

The cell culture was done using our recently published Gravitational Lumen Patterning (GLP) technique to form 3D cylindrical lumen within microchannels.³² This technique harnesses the control of the gravitational force, buoyant effect, and pressure difference across the microfluidic channel to form a monolayer of endothelial cells surrounded by multiple layers of muscle cells embedded in the extracellular matrix. In summary, the devices were first degassed within a vacuum chamber and then filled with an ice-cold mixture of LMCs and collagen (see next) followed by rotating the device for 90° and then adding an ice-cold cell medium to the device inlet. In this case, the cell medium would wash off the hydrogel and make 3D cylindrical structures within the microfluidic channel. By rotating the devices, we set the gravitational force in parallel to the microfluidic channel's axial direction so that the liquid with higher density (hydrogel) cannot push the liquid with lower density (cell medium) towards the top of the channel before hydrogel polymerization. Thus, we achieve a symmetrical lumen in which the muscle layer thickness is almost consistent at different angles around the lumen crosssection. The devices were kept in a 37 °C incubator for nearly 40 minutes followed by extensive perfusion of cell medium to wash off all undesired chemicals that remained within the polymerized hydrogel. For on-chip cell culture using GLP, LMCs were first trypsinized and mixed with rat tail type I collagen (9 mg ml⁻¹), mixed with the basal buffer (HEPES, NaHCO₃, NaOH) to reach the final concentration of 5×10^6 cells per ml with pH of 7.4. The cell-hydrogel mixture was then used in the GLP technique (described previously) to form 3D lumen within the microfluidic devices. For devices with no LMCs, only the hydrogel mixture was perfused within the channels before making the lumen using GLP. After waiting one day for LMCs to properly attach and proliferate within the ECM, LECs were trypsinized and mixed with the co-culture medium (1:3 LMC: LEC medium) with the final concentration of 2.5×10^6 cells per ml and were consequently seeded on the inner lumen layer in four steps (40 minutes for each lumen side) to form endothelium. The Lymphangion-Chip devices were kept at 37 °C and 5% CO₂ for nearly 3 days to be ready for the experiment while the co-culture medium was exchanged every 12 hours.

Flow control and intracellular calcium measurement

We used a pressure-driven flow system in this work (Elveflow). When the confluent endothelial layer was observed using phase-contract microscopy, for each device, the average lumen inner diameter was calculated by measuring the diameter in three different locations (one near inlet, one near outlet, and one in the middle). Considering laminar incompressible parabolic flow within the cylindrical lumen, the needed flow rate was calculated using the Hagen-Poiseuille equation based on the target luminal wall shear stress and average lumen inner

diameter.³⁶ For each device, the resulting flow profile was produced using our microfluidic pump (Elveflow). Then, the devices were washed with Phosphate-buffered saline (PBS). We loaded the devices with Fluo-4 calcium imaging solution (1% PowerLoad concentrate, 0.1% Fluo-4-AM, 89.9% PBS, ThermoFisher) and incubated at 37 °C for 1 hour. Later, the Fluo-4 solution was washed off the devices extensively with PBS, followed by filling the channels with phenol-red free high-glucose DMEM-F12 (Gibco). At this stage, the devices were ready for the experiment.

The tubing of the pressure pump was connected to the inlet and outlet of the channel and the device was placed inside a stage top incubator (Tokai Hit, Japan) to keep the cells in 5% CO₂ and 37 °C during the experiment. The stage top incubator was placed under the optical lens of the Zeiss Axio Observer Z1 inverted setup (LD Plan Neofluar, 20×, NA 0.4). Devices were kept in no-flow condition for at least 10 minutes prior to the experiment. The 15 ml Falcon tubes containing cell medium were kept in a 37 °C water bath to keep cell medium warm while flowing within the devices. The microscope lens was set to zoom on either LMCs or LECs (identified based on morphology and location) and fluorescent images were captured with 494 nm excitation wavelength every 15 s and 0.5 s for step and oscillatory shear experiments, respectively.

Data processing, curve fitting, and signal analysis

Raw images were processed using ImageJ Fiji. For each experiment, multiple regions of interest (~10-20 ROIs) were selected each containing a single cell. At each time point, the background noise was collected based on an area with no cell and subtracted from all ROIs. The depth of field for our imaging setup was calculated as 5.8 µm, for a light wavelength of 460 nm. Since we performed the calcium analyses from LMCs that were on average 50-100 µm far from endothelium (>10× of 5.8 µm depth of field), our microscope did not pick much background from LEC. However, to eliminate the remaining background noise, the plug-in noise reduction module of ImageJ was used. The calcium level at each time point (F_t) was measured by averaging the fluorescent intensities measured from all ROIs. The basal calcium level (F_0) was calculated by averaging the calcium level data between the last 4 time points before starting the flow. The data were corrected for photobleaching using the exponential fitting method.³⁷ In brief, the total intensity value of all time points was curve-fitted with an exponential decay curve. Then, the decay curve was used to calculate the true fluorescent intensity of each time point. Finally, the normalized intracellular calcium level was calculated as:

$$\label{eq:normalized} \text{Normalized intracellular calcium level} = \frac{F_{\text{t}}}{F_{0}}.$$

To further analyze the oscillatory shear-mediated calcium signal, the raw fluorescent data was curve fitted with cubic spline technique (MATLAB vR2020a), because it preserves the behavior and characteristic of the original signal.³⁸ Later, the first-order polynomial fit was performed on the processed signal to obtain the baseline, and then the secondary oscil-

latory signal was calculated by subtracting the baseline from the spline curve-fit signal.³⁹ To convert the signal from the time domain to the frequency domain, fast Fourier transform analysis (FFT) was applied to data.⁴⁰ First, the Fourier transform of the signal was computed. Later, the two-sided and single-sided spectrums of the signal were formed in the sequence based on even-valued signal length. Finally, the single-sided amplitude spectrum was scanned to obtain the dominant frequency of the original signal.

Immunohistochemistry

We performed the immunohistochemistry by starting with standard fixation (4% paraformaldehyde, Sigma) for 20 minutes at room temperature followed by 10 minutes of permeabilization (0.5% Triton X-100, Sigma). Then, we blocked the devices for 30 minutes (10% Bovine Serum Albumin, ThermoFisher Scientific). Later, the fixed devices were incubated with 1:100 dilution of mouse or rabbit primary antibodies for 90 minutes, including α -smooth muscle actin (α -SMA, eBioscience), vascular endothelial-cadherin (VE-cadherin, Invitrogen), or Lymphatic vessel endothelial hyaluronan receptor 1 (LYVE1, Invitrogen) followed by 60 minutes of incubation with secondary anti-mouse or antirabbit fluorescent antibodies (invitrogen, 1:200 dilution). Finally, cell nuclei were stained with Hoechst 33258 (invitrogen, 1:2000 dilution).

Statistical analysis

GraphPad v9 was used for statistical analysis. The graph bars are shown as the mean value while the error bars are represented as the standard error of the mean (SEM). To compare two data sets within the same group, we used Student's t-test. Meanwhile, to compare two data groups, we used analysis of variance (ANOVA) with post-hoc correction to determine whether there is a significant difference between the means of the independent groups. We considered P < 0.05 as the threshold for demonstrating the significant difference. The normality of data was also tested with Shapiro–Wilk test.

Results and discussion

Intracellular calcium dynamics in response to step shear

Relative to blood vessels, the lymphatic vessels experience sudden shear transients due to the complex lymph transport. These instant shear changes vary significantly in different physiological and pathophysiological conditions. LECs dynamically alter their morphology and barrier function in response to these sudden changes in shear stress that often determines progression and outcome of pathology. Therefore, we initiated our experiments by exposing Lymphangion-Chip to step shear (*i.e.*, step flow profile) for generating instant shear change applied to the endothelium. After connecting the flow control system and preparing the imaging setup (see Methods), the devices were kept under no shear for 5 minutes (0–5 min) followed by an instant step

increase in shear rate. Then, the devices were kept in constant shear for 10 minutes followed by a 5 minutes "resting" period in which the flow rate was set back to zero (Fig. 2A). When we analyzed the LECs, we observed that upon initiating the shear pulse for 10 min (5-15 min), the normalized intracellular calcium level $[Ca^{2+}]_i$ elevated gradually to a maximum value followed by a gradual decay back towards the baseline value (ESI Video 2†). This calcium signaling dynamics was observed within the time when the shear rate spike stayed constant. After setting the shear value back to zero at 15 min, the decay in the calcium signal was persistent until the calcium level recovered and reached back to the basal value. We found this trend for the entire range of shear values we applied. These trends in data from the co-cultured Lymphangion-Chip are consistent with observations made in prior studies in LEC monolayers.22 However, in this device, we also investigated for the first time, these calcium dynamics within the muscle cells. We found a similar rise and fall trend of intracellular [Ca²⁺]_i within the LMCs across the range of shear applied (Fig. 2C and ESI Video 3†). Interestingly, relative to the LECs, the magnitudes of intracellular [Ca2+]i was truncated. We also made devices with LMC monoculture and measured the intracellular calcium content of LMCs both close to the lumen boundary and away from the flow field while exposing the devices to a

step shear profile (10 dyne per cm²). LMCs that were closer to the lumen boundary and could sense the shear showed an elevation in their cytosolic calcium content. However, LMCs that were cultured away from the flow field (about 50–100 μm from the lumen boundary) did not show a significant change in their cytosolic calcium level (ESI Fig. 1†). Overall, these data demonstrate that LMCs also respond to the intraluminal shear stress applied to the LECs, possibly through the mechanosignaling within the LECs.

When we quantitatively analyzed the data of intracellular $[Ca^{2+}]_i$ across the shear values for both LECs and LMCs, we observed that the maximum normalized level of calcium was directly proportional to the shear rate magnitude for both cell types (Fig. 3A and B). For instance, applying the step shear of 10 dyne per cm² resulted in an increase of 19.8% in cytosolic calcium level of LECs in co-culture. Meanwhile, the rise in LECs calcium level in co-culture was 11.0% and 4.4% for 1 and 0.1 dyne per cm² shear stress, respectively (Fig. 3A). The intracellular calcium level $[Ca^{2+}]_i$ for LMCs in co-culture was also shear-dependent, similar to that observed in LECs, starting from 2.3% increase in 0.1 dyne per cm² up to 10.0% increase in 10 dyne per cm² (Fig. 3B), revealing that both the LECs and LMCs are responsive to shear, and also reinforcing that the Lymphangion-Chip is able to serve as an experimental system

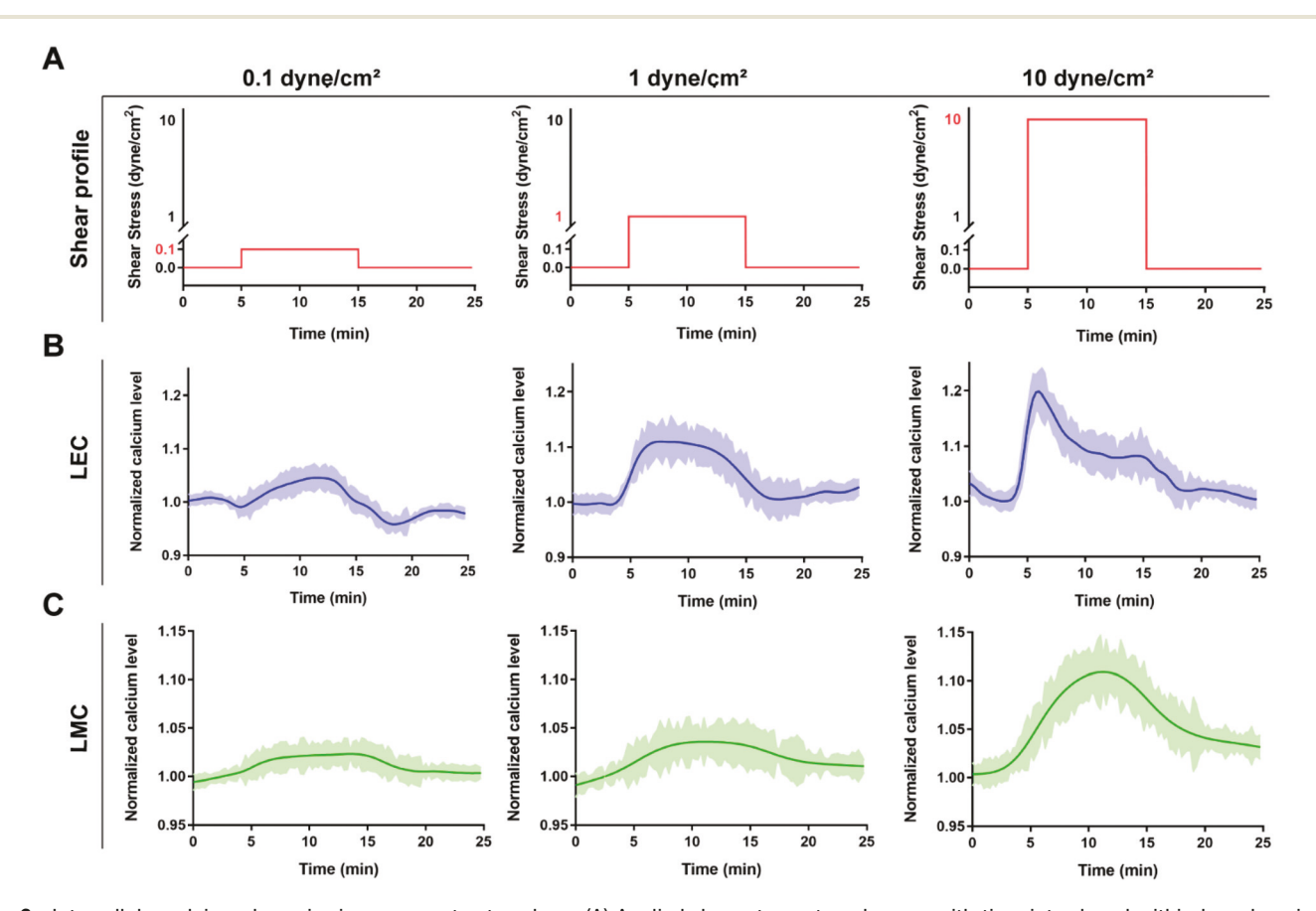


Fig. 2 Intracellular calcium dynamics in response to step shear. (A) Applied shear stress step changes with time introduced within Lymphangion-Chip at variable amplitudes. Normalized intracellular calcium level of (B) lymphatic endothelial cells (LEC) and (C) lymphatic muscle cells (LMC). Shaded color shows the 95% confidence interval band; n = 7 for all experiments.

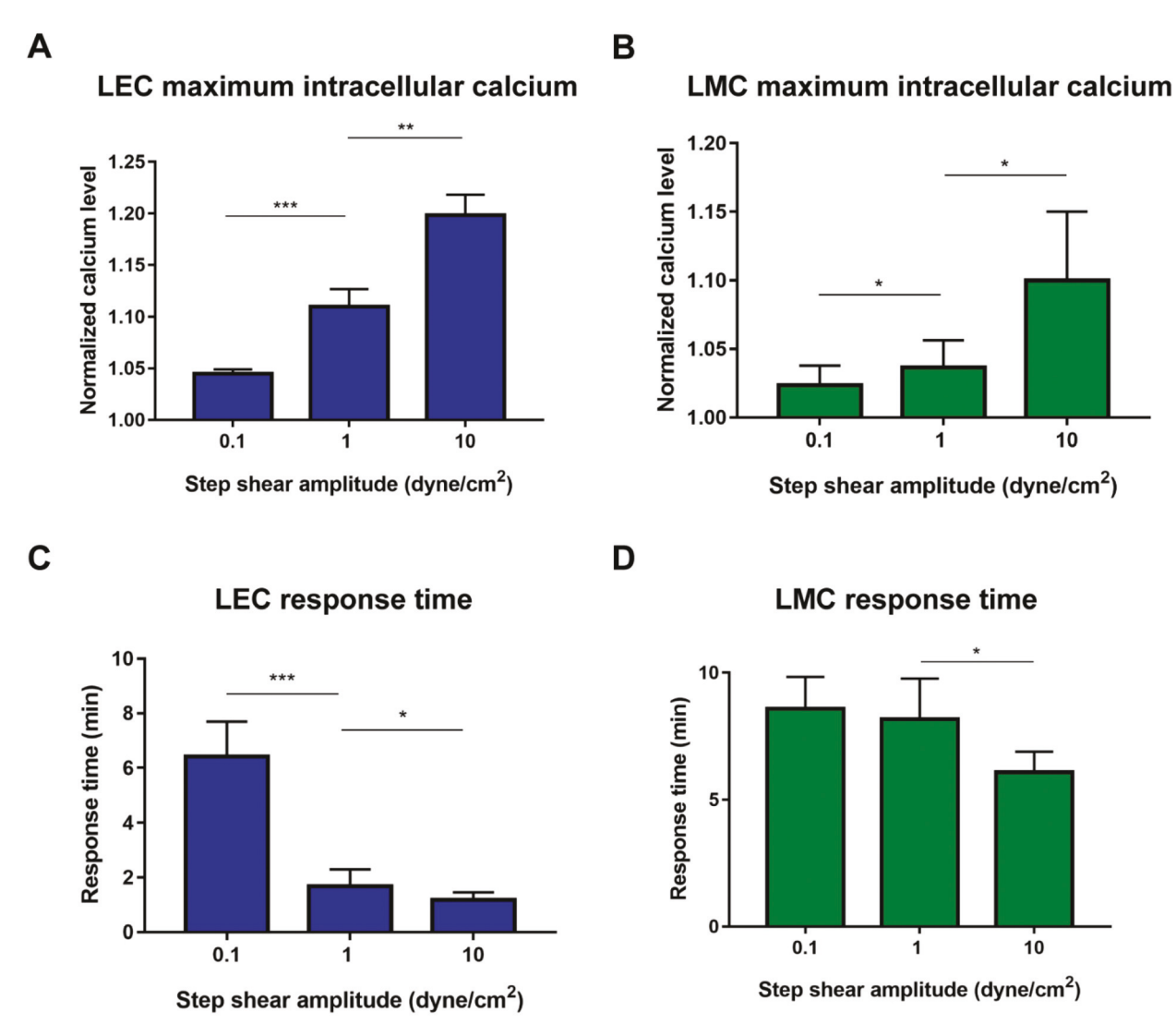


Fig. 3 Maximum intracellular calcium and response time due to step shear. Step changes in shear induced, maximum intracellular calcium in (A) LECs, and (B) LMCs. Step changes in shear induced, response time in (C) LECs, and (D) LMCs. *p < 0.05, **p < 0.005, **p < 0.001; n = 5-7 for all the experiments.

to investigate calcium-dependent mechanobiology in a typical lymphatic vessel. In most cell types, the Ca²⁺ balance within the cytoplasm alternates instantly and transitionally since pumps in the endoplasmic reticulum and plasma membrane continually remove Ca2+ from the cytoplasm.44,45 Therefore, the average cytosolic calcium concentration is not the only crucial parameter in calcium signaling and the duration of the individual Ca²⁺ pulses and how rapid the intracellular calcium reaches the desired level also play a major role in providing the cell with the opportunity to encode multiple forms of information. 45,46 Therefore, as another relevant metric of these dynamics, we defined a parameter named "response time" which is the time (in minutes) between initiating the flow (i.e., shear) and reaching the calcium peak. By elevating the shear amplitude, we observed a significant reduction in LEC response time from 6-8 minutes in 0.1 dyne per cm² to nearly 1 minute in 10 dyne per cm² (Fig. 3C). Same as LECs, the

LMCs response time was also inversely proportional with step shear amplitude (Fig. 3D). Notably, we found that at physiological or low shear steps, the response times for both LEC and LMC are nearly the same, but at high shear, the LECs have a quicker response rate relative to the LMCs whose response time was conserved. This suggests that since LECs interface with the flow directly, they can quickly respond to sharp changes in shear, but LMCs possibly sense these mechanical signals through the LECs which is more conserved and time-dependent. LECs are known to be responsive to flow alterations both temporally and spatially.⁴⁷ However very few studies have evaluated its effects directly on LMCs. In blood vessels, endothelial-derived hyperpolarization, caused by an elevation in the intracellular Ca²⁺ concentration, ^{15,16} functions as a signaling pathway between ECs as well as ECs and SMCs. Thus, ECs and SMCs are coupled electrically leading to vasodilation and contractile modulation. 21,48 However, LECs are

shown to lack the Ca²⁺-activated K⁺ channels which result in depolarization (rather than hyperpolarization) in the lymphatics endothelium. In addition, LECs are shown to be electrically decoupled from LMCs which is believed to result in efficient conduction of contraction waves in the adjacent LMCs that are required for propulsive lymph flow.²⁶ Our data with Lymphangion-Chip shows that LECs and LMCs are coupled through calcium dynamics. Since calcium and electriof vasculature are cal dynamics shown interconnected, 49,50 some form of electrical coupling may potentially exist also between the lymphatic vascular cells. More rigorous experiments and biological studies are needed to investigate this possibility.

Intracellular calcium dynamics in response to pulsatile shear

Transporting lymphatic vessels (lymphangions) have valves that pump the lymph such that the flow rate exhibits an oscillatory pattern with a period of 3–9 seconds.^{7,31,51} Even though there are a few numerical studies for Calcium and NO dynamics in oscillatory flow within lymphatics,²³ prior experimental work has not fully investigated calcium dynamics in pulsatile flow conditions.^{22,26,52} Thus, we were inspired to direct our Lymphangion-Chip to also reveal how pulsatile flow may influence intracellular calcium [Ca²⁺]_i dynamics. An

average shear stress of ~0.5-1 dyne per cm² with a peak of up to 10 dyne per cm² is regularly observed in lymphatic vessels in vivo. 31,51,53-55 Using a programmed microfluidic pressure pump, we next introduced flow profiles with the frequency of 10 sinusoidal pulses per min (6 s period) and three shear amplitudes of 0.1, 1, and 10 dyne per cm² to model lymphatics in inflammatory, normal, and supraphysiological conditions, respectively (Fig. 4A). When the pulsatile shear profile was introduced from baseline uniform flow (5 min), we observed that the general trend of intracellular calcium [Ca²⁺]_i was elevated in both the LECs (Fig. 4B) and LMCs (Fig. 4C) for a few minutes. In LECs however, this increase was more prominent than in LMCs. In the lower shear rates of 0.1 and 1 dyne per cm², LMCs demonstrated a relatively lower shear-mediated calcium sensitivity compared to LECs. However, when the vessel's endothelium was exposed to the higher shear amplitude of 10 dyne per cm², LMCs expressed the same exponential rise and fall in calcium dynamics as LECs (Fig. 4C). However, in both cell types, the overall trend in intracellular calcium [Ca²⁺]_i also decayed gradually to a near basal level. This suggested that an onset of pulsatile flow would raise the calcium but eventually result in a constant average intracellular calcium $[Ca^{2+}]_i$ level in both the LECs and LMCs. Like before, when we quantitatively analyzed the data of intracellu-

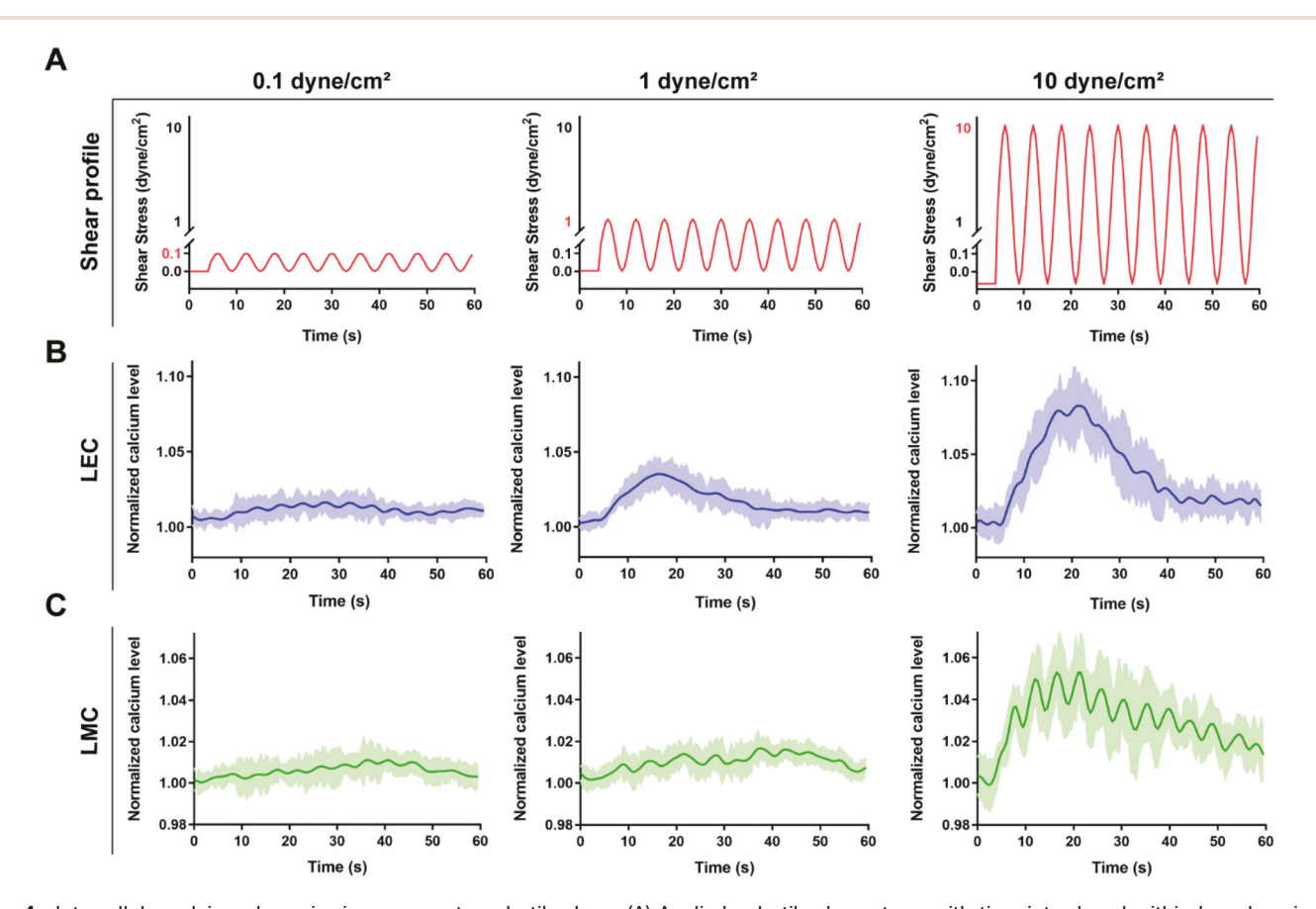


Fig. 4 Intracellular calcium dynamics in response to pulsatile shear. (A) Applied pulsatile shear stress with time introduced within Lymphangion-Chip at variable amplitudes. Normalized intracellular calcium level of (B) lymphatic endothelial cells (LECs) and (C) lymphatic muscle cells (LMCs). Shaded color shows the 95% confidence interval band; n = 7 for all experiments.

lar $[Ca^{2^+}]_i$ across the shear values for both LECs and LMCs, we observed that the maximum normalized level of calcium was directly proportional to the amplitude of pulsatile flow for both cell types (Fig. 5A and B). Due to the lower shear amplitude of 0.1 dyne per cm², LEC intracellular calcium increased only modestly while 10 dyne per cm² shear magnitude resulted in significantly high elevation in LEC $[Ca^{2^+}]_i$. Likewise, LMCs maximum normalized intracellular $[Ca^{2^+}]_i$ increased directly proportional to pulsatile shear amplitude (Fig. 5B). When we analyzed the response time, we saw that within the LECs, there

was a small drop in response, when the amplitude was raised from 0.1 to 1 dyne per cm² (Fig. 5C). But it was increased drastically when 10 dyne per cm² was applied. In contrast, within the LMCs, there was a small and then a more prominent drop in intracellular calcium [Ca²⁺]_i as amplitude was raised respectively (Fig. 5D). We suspect that the supraphysiological value of 10 dyne per cm² models the shear applied to LECs around valve leaflets that is two to three times higher than downstream straight segments and causes a major shift in calcium response time compared to lower shear amplitudes.⁵⁶

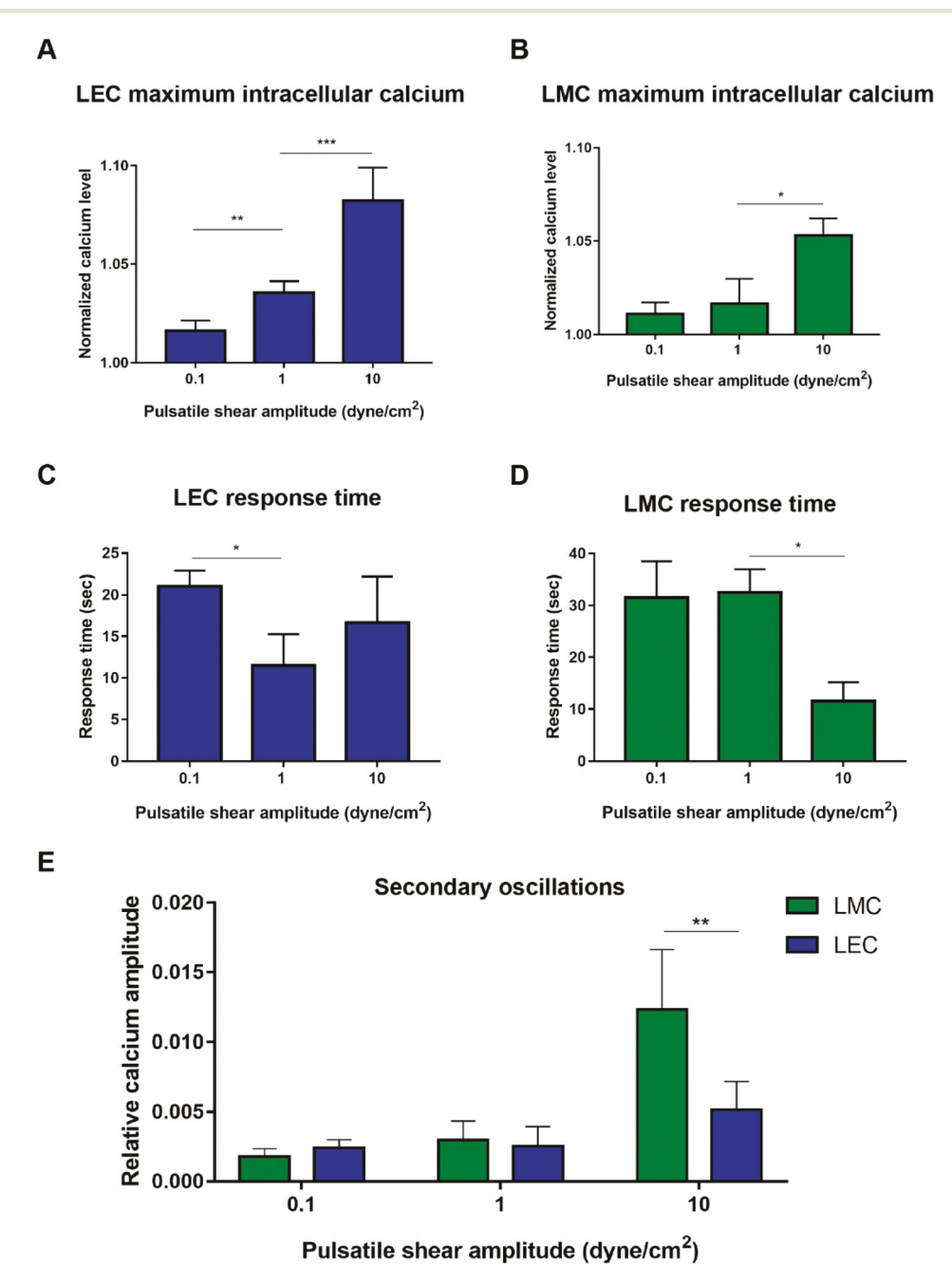


Fig. 5 Maximum intracellular calcium and response time due to pulsatile shear. Pulsatile flow induced, maximum intracellular calcium in (A) LECs, and (B) LMCs. Pulsatile flow induced, response time in (C) LECs, and (D) LMCs. (E) Average amplitude of LEC and LMC secondary calcium oscillations under pulsatile shear. *p < 0.05, **p < 0.005, **p < 0.001; n = 5–7 for all the experiments.

However, the average LMC contractile function is shown to be consistent irrespective of their location within lymphangion which explains the shear-dependent decrease in LMCs response time even in higher shear amplitudes.⁵⁷ Moreover, several mechanosensors are shown to play a role in sheardependent calcium dynamics including membrane receptors,58 matrix adhesion proteins,59 glycocalyx,60 and plasma membrane channels. 61 However, the role of each of these regulators in mediating the responses observed in the lymphatics is yet to be determined.⁶² There is a possibility for a calcium inhibitory pathway that contributes more effectively in high pulsatile shear which increases in LEC calcium response time. Future studies using our platform may allow such hypotheses to be tested. It is also noteworthy that at a shear of 0.1 dyne per cm² that is representative of hydrodynamic conditions observed in lymphedema, the response time in LECs and LMC calcium dynamics was significantly high. This observation could partially explain the buildup of interstitial fluid in edema and associated conditions. As flow gets impaired in lymphedema, a considerable delay would be produced in LEC calcium response which results in even more delayed LMC contractile function resulting in a positive feedback and pathological condition.

Interestingly, unlike in the step shear condition, we observed that in addition to the rise and fall in intracellular calcium [Ca²⁺]_i, a set of secondary oscillations were also present within the signal amongst both the LECs and the LMCs. We found that the secondary oscillations observed in the original signal for 0.1, 1, and 10 dyne per cm² shear amplitudes have almost the same frequency as the input shear profile (0.167 Hz) (Table 1). Therefore, these data from the Lymphangion-Chip predict that calcium signaling in vivo may have the same frequency as of the flow. But rapid changes in amplitude and other bulk flow conditions may result in an overall intracellular calcium [Ca²⁺]_i response where it may increase rapidly and decline gradually, keeping the local oscillation frequency conserved. This also demonstrates the high sensitivity of calcium channels and the crucial role of pulsatile shear rate in calcium-operated functions of lymphatics such as permeability and contraction. By analyzing the calcium signal amplitude in LMCs and LECs, it appears that the LMCs are significantly more sensitive than LECs while the Lymphangion-

Table 1 Secondary oscillations in intracellular calcium dynamics. Local secondary frequencies in intracelleular calcium for LECs and LMCs are shown for different pulsatile shear amplitudes. The output frequencies for all different conditions are near the input shear frequency of 0.167 Hz (6 s period). n = 5-7 for all the experiments

Pulsatile shear amplitude (dyne per cm²)	Calcium frequency (Hz)	
	LEC	LMC
0.1	0.162 ± 0.007	0.166 ± 0.008
1	0.132 ± 0.022	0.139 ± 0.019
10	0.163 ± 0.012	0.168 ± 0.006
	Input shear frequency = 0.167	

Chips were exposed to a high pulsatile shear (10 dyne per cm² amplitude) which suggests that cytoplasm calcium sources and plasma membrane calcium channels could be more active within LMCs compared to LECs (Fig. 5E). We also observed that the average phase difference between input pulsatile shear and output calcium signal was 2.3 s and 4 s for LECs and LMCs, respectively. This nearly 2 s of lag between LECs and LMCs suggests that LEC-LMC crosstalk may be influenced by the transport of soluble factors between the two cell types, which may be evaluated in future. In most animal models, the lymphatic vessel is shown to exhibit phasic and tonic contractions, which this model did not specifically focus on. Therefore, our results are foundational to the opportunity to assess contractile behavior through mechanobiological signaling with the Lymphangion-Chip.

Contribution of lymphatic muscle cell in endothelial calcium dynamics

A significant feature of the Lymphangion-Chip is that it allows a reductionist approach in studying vascular physiology. Leveraging this aspect, we focused on identifying the specific contribution of the presence of LMCs in the shear-dependent intracellular calcium [Ca²⁺]_i response amongst the LECs. The lumen cross-section was slightly elliptical, regardless of monoculture of LMC or a co-culture with LECs. In particular, the ratio of the lumen height (b) over lumen width (a) (i.e., b/a) was consistent with or without LMCs (ESI Fig. 2†). Thus, we could exclude the LMCs from the system without change in shape or shear stress distribution within the device. We found that in the absence of the LMCs, that is, monoculture of the LECs, when step changes in flow were introduced the LECs intracellular calcium [Ca2+]i was inhibited compared to when we co-cultured LECs with LMCs. By increasing the step shear value within Lymphangion-Chips, we observed a more significant difference in LEC intracellular calcium [Ca²⁺]_i between monoculture and co-culture conditions. For instance, the difference between normalized LECs intracellular calcium [Ca²⁺]_i in monoculture versus co-culture in 10 dyne per cm² was five-fold more than in 0.1 dyne per cm² (Fig. 6A). Overall, due to the significant differential response in calcium dynamics when LECs were in monoculture versus co-culture with LMCs, the data suggests that LMCs influence the calcium dynamics and related mechanosignaling within the LECs.

Secondly, the LECs response time in all 3 step shear values was reduced in co-culture with LMCs compared to monoculture (Fig. 6B). This difference is significant at physiological step shear of 1 dyne per cm², but not under edemagenic low shear or high shear. When pulsatile flow was introduced, we found the same trend in LECs maximum intracellular calcium and response time so that LECs in monoculture (no LMCs) responded slower and with a reduced calcium peak value compared to LECs co-cultured with LMCs (Fig. 6C and D). Our results show that upon co-culture with LMCs, the endothelial intracellular calcium content and influx rate increases significantly compared to its monoculture. The molecular underpinnings of this shear-dependent phenomenon are beyond the

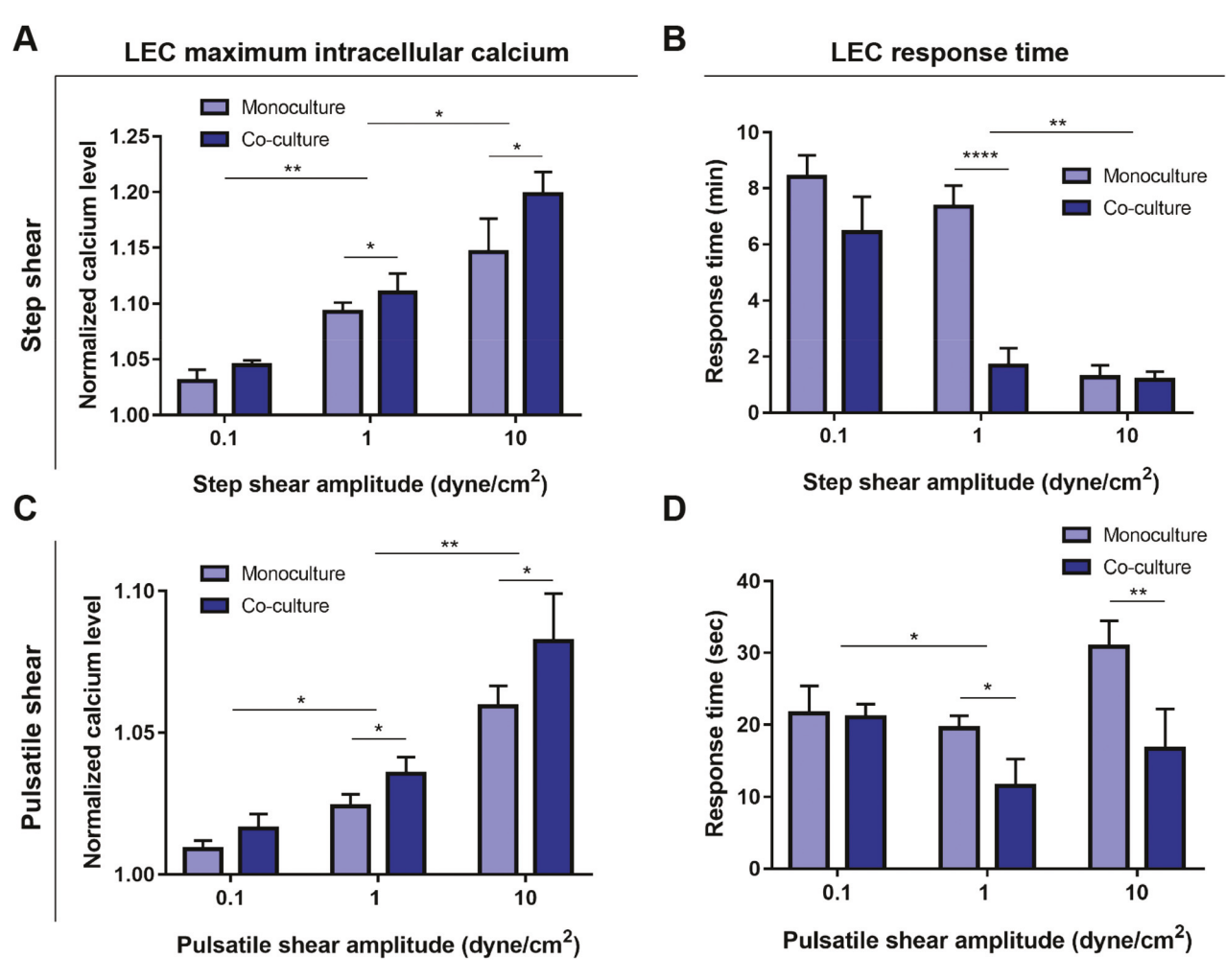


Fig. 6 Contribution of LMCs in LEC calcium dynamics. Step changes in shear induced, (A) maximum intracellular calcium and (B) response time in LECs under monoculture or co-culture with LMCs. Pulsatile shear induced, (C) maximum intracellular calcium and (D) response time in LECs under monoculture or co-culture with LMCs. *p < 0.005, **p < 0.005, **p < 0.001; n = 5-7 for all the experiments.

scope of this work, but Lymphangion-Chip provides a tool for scientists to investigate mechanisms of LEC-LMC crosstalk at the molecular and cellular level.

Conclusions

The combination of intrinsic and extrinsic contractility of the lymphatic vessels subjects them to a unique mechanical microenvironment regulated by multiple fluid forces that differentiates them from the blood vasculature. It is known that amongst the blood and lymphatic vascular cells, select membrane proteins convert extracellularly applied mechanical stimuli into intracellular calcium signals. These and other chemical signals also operate by opening/closing channels formed by their transmembrane domains (TMDs) to drive the movement of molecules across the cell membrane, ultimately guiding cellular response to mechanical forces. In lymphatics, this interplay of mechanical forces and resulting mechanosensing through intracellular calcium is expected to be unique

because the lymph hydrodynamics are pulsatile and low shear, but may undergo rapid changes in amplitude due to lymphatic valve pumping, and other inflammatory signaling due to the extensive immune cell transport that undergoes within the lymphatics. Therefore, intracellular calcium can be an effective analytical mechanosensor of lymphatic function. Our Lymphangion-Chip is a microphysiological platform that supports co-culture of the axially-aligned vascular endothelial and transversally wrapped mural cells under precisely controlled environmental fluid mechanical forces, as only seen in vivo in the past. Here, we deployed this system to systematically characterize the independent and interdependent intracellular calcium dynamics of the LECs and the LMCs. Our observation of the shear-dependent decrease in LECs response time and the significant difference between step and oscillatory flow profiles indicates the crucial rule of cyclic mechanical forces in calcium dynamics and responsiveness of these vascular cells, and thus in regulating critical lymphatic functions. In contrast to blood vessels reported in some studies, 63 we found the possibility of the electrical coupling of the LECs and LMCs

which results in a reduction of the response time upon coculture. However, more experiments are needed to validate the direct relation between electrical and calcium coupling in this context. This may govern lymphatic vasodilation and permeability through signaling pathways that may now be explored with this platform in the future. Lymphangion-Chip platform can also be deployed in future studies to reveal the molecular signaling pathways between the two cell types and compare the relative contributions of flow and chemical signaling.

Moreover, we recorded secondary calcium oscillations within both LECs and LMCs under pulsatile flow. The impact and consequence of these oscillations in lymphatic contractile function, lymph transport and other physiological responses to external cues is unclear, and has not been a focus in the *in vivo* studies so far. Therefore, these *in vitro* intracellular calcium dynamics of LEC and LMCs observed in a co-culture setting may also complement and provoke more *in vivo* studies directed at the understanding of the unique adaptation mechanism shown by both of these cell types in response to lymph flow and stasis observed in pathological conditions such as secondary lymphedema.

Author contributions

A. S. performed the microfluidics experiments. A. S. and A. J. designed the experiments, analysed results, made the figures, and wrote the paper with feedback from all authors; S. C., and M. M. isolated and characterized the lymphatic endothelial and muscle cells used in this study, and D. C. Z. contributed to data analysis.

Conflicts of interest

The authors declare no conflict of interest.

Acknowledgements

We thank Dr S. Vitha at the Microscopy and Imaging Center at Texas A&M University for assisting with confocal imaging. This project was supported by the NHLBI of NIH under Award Number R01HL157790, NIBIB of NIH under Award Number R21EB025945, NSF CAREER Award number 1944322, Texas A&M Engineering, and President's Excellence in Research Funding Award of Texas A&M University to A. J; AHA Scientist Development Grant 17SDG33670306 and CPRIT grant RP210213 to S. C.

References

1 M. A. Swartz, The physiology of the lymphatic system, *Adv. Drug Delivery Rev.*, 2001, **50**(1–2), 3–20.

2 W. L. Olszewski, The lymphatic system in body homeostasis: physiological conditions, *Lymphatic Res. Biol.*, 2003, 1(1), 11–24.

- 3 T. V. Petrova and G. Y. Koh, Biological functions of lymphatic vessels, *Science*, 2020, **369**(6500), eaax4063.
- 4 S. G. Rockson and K. K. Rivera, Estimating the population burden of lymphedema, *Ann. N. Y. Acad. Sci.*, 2008, **1131**(1), 147–154
- 5 S. G. Rockson, The lymphatics and the inflammatory response: lessons learned from human lymphedema, *Lymphatic Res. Biol.*, 2013, 11(3), 117–120.
- 6 Y. Yuan, *et al.*, Modulation of immunity by lymphatic dysfunction in lymphedema, *Front. Immunol.*, 2019, **10**, 76.
- 7 D. C. Zawieja, Contractile physiology of lymphatics, *Lymphatic Res. Biol.*, 2009, 7(2), 87–96.
- 8 M. J. Davis, *et al.*, Intrinsic increase in lymphangion muscle contractility in response to elevated afterload, *Am. J. Physiol.: Heart Circ. Physiol.*, 2012, **303**(7), H795–H808.
- 9 A. A. Gashev and D. C. Zawieja, Hydrodynamic regulation of lymphatic transport and the impact of aging, *Pathophysiology*, 2010, 17(4), 277–287.
- 10 J. A. Kornuta, *et al.*, Effects of dynamic shear and transmural pressure on wall shear stress sensitivity in collecting lymphatic vessels, *Am. J. Physiol.: Regul., Integr. Comp. Physiol.*, 2015, **309**(9), R1122–R1134.
- 11 A. A. Gashev, M. J. Davis and D. C. Zawieja, Inhibition of the active lymph pump by flow in rat mesenteric lymphatics and thoracic duct, *J. Physiol.*, 2002, **540**(3), 1023–1037.
- 12 A. M. Andrews, *et al.*, Direct, real-time measurement of shear stress-induced nitric oxide produced from endothelial cells in vitro, *Nitric Oxide*, 2010, 23(4), 335–
- 13 M. Kuchan and J. Frangos, Role of calcium and calmodulin in flow-induced nitric oxide production in endothelial cells, *Am. J. Physiol.: Cell Physiol.*, 1994, **266**(3), C628–C636.
- 14 M. B. Dancu, *et al.*, Atherogenic endothelial cell eNOS and ET-1 responses to asynchronous hemodynamics are mitigated by conjugated linoleic acid, *Ann. Biomed. Eng.*, 2007, 35(7), 1111–1119.
- 15 M. Kuchan and J. Frangos, Shear stress regulates endothelin-1 release via protein kinase C and cGMP in cultured endothelial cells, *Am. J. Physiol.: Heart Circ. Physiol.*, 1993, 264(1), H150–H156.
- 16 R. O. Dull and P. Davies, Flow modulation of agonist (ATP) response (Ca2+) coupling in vascular endothelial cells, *Am. J. Physiol.: Heart Circ. Physiol.*, 1991, **261**(1), H149–H154.
- 17 J. Shen, *et al.*, Fluid shear stress modulates cytosolic free calcium in vascular endothelial cells, *Am. J. Physiol.: Cell Physiol.*, 1992, **262**(2), C384–C390.
- 18 K. A. Gerhold and M. A. Schwartz, Ion channels in endothelial responses to fluid shear stress, *Physiology*, 2016, 31(5), 359–369.

19 M. Félétou, Endothelium-dependent hyperpolarization and endothelial dysfunction, *J. Cardiovasc. Pharmacol.*, 2016, **67**(5), 373–387.

- 20 C. J. Garland and K. A. Dora, EDH: endothelium-dependent hyperpolarization and microvascular signalling, *Acta Physiol.*, 2017, 219(1), 152–161.
- 21 P. Bagher and S. S. Segal, Regulation of blood flow in the microcirculation: role of conducted vasodilation, *Acta Physiol.*, 2011, 202(3), 271–284.
- 22 M. Jafarnejad, *et al.*, Measurement of shear stress-mediated intracellular calcium dynamics in human dermal lymphatic endothelial cells, *Am. J. Physiol.: Heart Circ. Physiol.*, 2015, **308**(7), H697–H706.
- 23 C. Kunert, *et al.*, Mechanobiological oscillators control lymph flow, *Proc. Natl. Acad. Sci. U. S. A.*, 2015, **112**(35), 10938–10943.
- 24 D. Choi, *et al.*, Laminar flow downregulates Notch activity to promote lymphatic sprouting, *J. Clin. Invest.*, 2017, 127(4), 1225–1240.
- 25 V. N. Surya, *et al.*, Lymphatic endothelial cell calcium pulses are sensitive to spatial gradients in wall shear stress, *Mol. Biol. Cell*, 2019, **30**(7), 923–931.
- 26 E. J. Behringer, *et al.*, Calcium and electrical dynamics in lymphatic endothelium, *J. Physiol.*, 2017, **595**(24), 7347–7368.
- 27 S. D. Zawieja, *et al.*, Differences in L-type Ca2+ channel activity partially underlie the regional dichotomy in pumping behavior by murine peripheral and visceral lymphatic vessels, *Am. J. Physiol.: Heart Circ. Physiol.*, 2018, 314(5), H991–H1010.
- 28 J. A. Castorena-Gonzalez, *et al.*, Mechanisms of connexinrelated lymphedema: a critical role for Cx45, but not Cx43 or Cx47, in the entrainment of spontaneous lymphatic contractions, *Circ. Res.*, 2018, 123(8), 964–985.
- 29 L. Munaron and M. Scianna, Multilevel complexity of calcium signaling: Modeling angiogenesis, *World J. Biol. Chem.*, 2012, 3(6), 121.
- 30 A. Mukherjee, *et al.*, entrainment of Lymphatic Contraction to oscillatory Flow, *Sci. Rep.*, 2019, 9(1), 5840.
- 31 C. Blatter, *et al.*, In vivo label-free measurement of lymph flow velocity and volumetric flow rates using Doppler optical coherence tomography, *Sci. Rep.*, 2016, **6**, 29035.
- 32 A. Selahi, *et al.*, Lymphangion-chip: a microphysiological system which supports co-culture and bidirectional signaling of lymphatic endothelial and muscle cells, *Lab Chip*, 2022, 22(1), 121–135.
- 33 A. Jain, et al., Organ-on-a-chip and 3D printing as preclinical models for medical research and practice, in *Precision Medicine for Investigators, Practitioners and Providers*, Elsevier, 2020, pp. 83–95.
- 34 H. Hayes, *et al.*, Development and characterization of endothelial cells from rat microlymphatics, *Lymphatic Res. Biol.*, 2003, **1**(2), 101–119.
- 35 M. Muthuchamy, *et al.*, Molecular and functional analyses of the contractile apparatus in lymphatic muscle, *FASEB J.*, 2003, 17(8), 920–922.

36 B. R. Munson, et al., Fundamentals of fluid mechanics, John Wiley & Sons, 2014.

- 37 K. Miura, Bleach correction ImageJ plugin for compensating the photobleaching of time-lapse sequences., *F1000Research*, 2020, **9**(1494), DOI: **10.12688**/ **f1000research**.27171.1.
- 38 S. McKinley and M. Levine, *Cubic spline interpolation*, College of the Redwoods, 1998, vol. 45((1)), pp. 1049–1060.
- 39 F. Zhang, *et al.*, An Automatic Baseline Correction Method Based on the Penalized Least Squares Method, *Sensors*, 2020, **20**(7), 2015.
- 40 M. Cerna and A. F. Harvey, The fundamentals of FFT-based signal analysis and measurement. 2000, Application Note 041, National Instruments.
- 41 J. P. Scallan, *et al.*, Lymphatic pumping: mechanics, mechanisms and malfunction, *J. Physiol.*, 2016, **594**(20), 5749–5768.
- 42 J. E. Moore Jr. and C. D. Bertram, Lymphatic System Flows, *Annu. Rev. Fluid Mech.*, 2018, **50**(1), 459–482.
- 43 J. W. Breslin and K. M. Kurtz, Lymphatic endothelial cells adapt their barrier function in response to changes in shear stress, *Lymphatic Res. Biol.*, 2009, 7(4), 229–237.
- 44 D. E. Clapham, Calcium signaling, *Cell*, 2007, **131**(6), 1047–1058.
- 45 E. Smedler and P. Uhlén, Frequency decoding of calcium oscillations, *Biochim. Biophys. Acta Gen. Subj.*, 2014, **1840**(3), 964–969.
- 46 R. E. Dolmetsch, K. Xu and R. S. Lewis, Calcium oscillations increase the efficiency and specificity of gene expression, *Nature*, 1998, **392**(6679), 933–936.
- 47 E. Michalaki, *et al.*, Perpendicular alignment of lymphatic endothelial cells in response to spatial gradients in wall shear stress, *Commun. Biol.*, 2020, 3(1), 1–9.
- 48 G. G. Emerson and S. S. Segal, Electrical coupling between endothelial cells and smooth muscle cells in hamster feed arteries: role in vasomotor control, *Circ. Res.*, 2000, 87(6), 474–479.
- 49 R. Busse, *et al.*, Hyperpolarization and increased free calcium in acetylcholine-stimulated endothelial cells, *Am. J. Physiol.: Heart Circ. Physiol.*, 1988, 255(4), H965–H969.
- 50 N. M. Tsoukias, Calcium dynamics and signaling in vascular regulation: computational models, *Wiley Interdiscip. Rev.: Syst. Biol. Med.*, 2011, 3(1), 93–106.
- 51 C. Chong, *et al.*, In vivo visualization and quantification of collecting lymphatic vessel contractility using near-infrared imaging, *Sci. Rep.*, 2016, **6**(1), 1–12.
- 52 V. N. Surya, *et al.*, Sphingosine 1-phosphate receptor 1 regulates the directional migration of lymphatic endothelial cells in response to fluid shear stress, *J. R. Soc., Interface*, 2016, 13(125), 20160823.
- 53 S. Liao, *et al.*, Method for the quantitative measurement of collecting lymphatic vessel contraction in mice, *J. Microbiol. Methods*, 2014, **1**(2), e6.
- 54 J. B. Dixon, *et al.*, Measuring microlymphatic flow using fast video microscopy, *J. Biomed. Opt.*, 2005, **10**(6), 064016.

55 J. B. Dixon, *et al.*, Image correlation algorithm for measuring lymphocyte velocity and diameter changes in contracting microlymphatics, *Ann. Biomed. Eng.*, 2007, **35**(3), 387–396.

- 56 J. T. Wilson, *et al.*, Confocal image-based computational modeling of nitric oxide transport in a rat mesenteric lymphatic vessel, *J. Biomech. Eng.*, 2013, 135(5), 51005.
- 57 A. A. Gashev, Physiologic aspects of lymphatic contractile function: current perspectives, *Ann. N. Y. Acad. Sci.*, 2002, **979**, 178–187. discussion 188–96.
- 58 S. Gudi, J. P. Nolan and J. A. Frangos, Modulation of GTPase activity of G proteins by fluid shear stress and phospholipid composition, *Proc. Natl. Acad. Sci. U. S. A.*, 1998, 95(5), 2515–2519.

- 59 E. Tzima, *et al.*, A mechanosensory complex that mediates the endothelial cell response to fluid shear stress, *Nature*, 2005, 437(7057), 426.
- 60 J. M. Tarbell and E. E. Ebong, The endothelial glycocalyx: a mechano-sensor and-transducer, *Sci. Signaling*, 2008, **1**(40), pt8–pt8.
- 61 P. F. Davies, Flow-mediated endothelial mechanotransduction, *Physiol. Rev.*, 1995, 75(3), 519–560.
- 62 J. Ando and K. Yamamoto, Flow detection and calcium signalling in vascular endothelial cells, *Cardiovasc. Res.*, 2013, **99**(2), 260–268.
- 63 S. Budel, *et al.*, Role of smooth muscle cells on endothelial cell cytosolic free calcium in porcine coronary arteries, *Am. J. Physiol.: Heart Circ. Physiol.*, 2001, **281**(3), H1156–H1162.